Effect of thermally excited lattice vibrations on the thermodynamic stability of tungsten ditellurides WTe2 under high pressure: A first-principles investigation

A. Ektarawong, P. Tsuppayakorn-aek, T. Bovornratanaraks, Björn Alling and N. Kanchanavatee

The self-archived postprint version of this journal article is available at Linköping University Institutional Repository (DiVA):
http://urn.kb.se/resolve?urn=urn:nbn:se:liu:diva-172403

N.B.: When citing this work, cite the original publication.
Ektarawong, A., Tsuppayakorn-aek, P., Bovornratanaraks, T., Alling, B., Kanchanavatee, N., (2021), Effect of thermally excited lattice vibrations on the thermodynamic stability of tungsten ditellurides WTe2 under high pressure: A first-principles investigation, *Computational materials science*, 186, 110024. https://doi.org/10.1016/j.commatsci.2020.110024

Original publication available at:
https://doi.org/10.1016/j.commatsci.2020.110024

Copyright: Elsevier
http://www.elsevier.com/

Tweet

LINKÖPING UNIVERSITY

Effect of thermally excited lattice vibrations on the thermodynamic stability of tungsten ditellurides WTe_2 under high pressure: a first-principles investigation

A. Ektarawong,[1,2] P. Tsuppayakorn-aek,[1,2] T. Bovornratanaraks,[1,2] B. Alling,[3] and N. Kanchanavatee[4,*]

[1] *Extreme Condition Physics Research Laboratory, Physics of Energy Materials Research Unit, Department of Physics, Faculty of Science, Chulalongkorn University, Bangkok, 10330, Thailand*

[2] *Thailand Center of Excellence in Physics, Ministry of Higher Education, Science, Research and Innovation, 328 Si Ayutthaya Road, Bangkok 10400, Thailand*

[3] *Theoretical Physics Division, Department of Physics, Chemistry and Biology (IFM), Linköping University, SE-581 83 Linköping, Sweden*

[4] *Physics of Energy Materials Research Unit, Department of Physics, Faculty of Science, Chulalongkorn University, Bangkok, 10330, Thailand*

The thermodynamic stability as a function of pressure and temperature of three WTe_2 polytypes, *i.e.*, Td, 1T′, and 2H phases, is examined using first-principles calculations, where the temperature-dependent contributions, arising particularly from the lattice vibrations, are derived from the quasi-harmonic approximation. We find that the critical transition pressure to the 2H phase increases almost linearly with increasing temperature. Through the inspection of the phonon density of states, 2H−WTe_2 is dynamically stable not only at high pressure, but also at zero pressure, indicating possible existence of 2H−WTe_2 also at ambient conditions. On the other side, our results demonstrate that, at relevant temperature and pressure, the thermodynamic stability of 1T′−WTe_2 is comparable to that of Td−WTe_2, and further analysis reveals substantial similarities in terms of structural behavior between Td−WTe_2 and 1T′−WTe_2. These findings suggest not only that the two polytypes are likely to coexist in practical samples of WTe_2 due probably to grains/regions either with tiny difference in stress, for example, or with different growth history, but also that the designation of 1T′, having been regularly used to described the compound under pressure in the literature, might actually be a mixture of Td and 1T′ polytypes, whose WTe_2 layers laterally slide *via* low transition barrier induced probably by the applied pressure, resulting in the splitting of (101) and (113) peaks as observed in the diffraction experiments.

INTRODUCTION

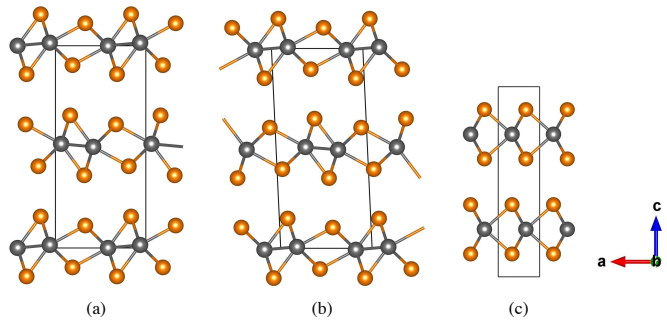

FIG. 1: Visualization of three stacking layered structures of WTe_2 viewed along the b axis: (a) Td phase, (b) 1T′ phase, and (c) 2H phase. The grey and orange spheres represent, respectively, W and Te atoms.

Tungsten ditelluride − WTe_2 − belonging to the family of layered transition metal dichalcogenides has recently received considerable interest from the materials research society. This can typically be attributed to its extremely large and non-saturating magnetoresistance at low temperature [1]. Furthermore, WTe_2 has been proposed as a candidate for the Type−II Weyl semimetals [2–4] and reported to display superconducting properties under high pressure [5–7]. In analogy to other transition metal dichalcogenides [8], WTe_2 crystallizes in the form of stacking layered structures, and for each individual layer of WTe_2, W atoms are sandwiched by and covalently bonded to Te atoms (see Fig. 1). Owing to the variation both in the stacking order of WTe_2 layers and in the atomic configuration of W and Te atoms constituting the layer, it is likely that different polytypes (or phase) of WTe_2 can exist. At ambient conditions, the orthorhombic structure with the space group of $Pmn2_1$ (Td phase), where both W and Te atoms occupy the Wyckoff positions $2a$, has been reported to be the most thermodynamically stable form of WTe_2, as depicted by Fig. 1(a) [9, 10], while the monoclinic structure with the space group of $P2_1/m$ (1T′ phase), where both W and Te atoms occupy the Wyckoff positions $2e$ (see Fig. 1(b)), has been demonstrated both by Lu *et al.* [7] and by Zhou *et al.* [11] *via* their experimental and theoretical studies to be thermodynamically favored over Td phase under high pressure ($p \gtrsim 4$ GPa). According to the findings in Ref. [7] and [11], the pressure-induced structural phase transition of WTe_2 from Td to 1T′ phases can be interpreted by the lateral sliding of adjacent layers of WTe_2, and such a transition has been suggested to be the origin of the observed superconducting behavior of WTe_2 at $T \lesssim 4$ K under high pressure. In addition to 1T′ phase, another high-pressure structure of WTe_2, crystallizing in the hexagonal lattice with the space group of $P6_3/mmc$

(2H phase), where W and Te atoms occupy the Wyckoff positions $2b$ and $4f$, respectively (see Fig. 1(c)), has been predicted to be thermodynamically stable with respect to 1T′ phase at $p \gtrsim 10$ GPa [7]. It has also been theoretically demonstrated that, instead of the Type-II Weyl semimetal, 2H phase of WTe_2 exhibits a semiconducting behavior at $p \lesssim 18$ GPa [7, 10]. It is, however, worth noting that, to the best of our knowledge, no successful synthesis of 2H−WTe_2 has so far been reported, although attempts to do so were made previously by Lu *et al.* [7] and Zhou *et al.* [11]. For example, as reported in Ref. [7], WTe_2 was compressed at $p = 15.4$ GPa using a diamond anvil cell and then laser-heated at $T > 2200$ K; however, the transition from 1T′ to 2H phases was not observed, and Lu *et al.* [7] have attributed this to a sluggish diffusion of W and Te atoms resulting from the high transition barrier between 1T′ and 2H phases, thus limiting the compound to access its thermodynamic equilibrium 2H phase in experiments. It should also be emphasized that the relative stability between 1T′−WTe_2 and 2H−WTe_2 as a function of pressure, as reported in Ref. [7], was evaluated without considering the effects of temperature, in particular lattice vibrations or phonons. Such thermally excited effects might, however, play a crucial role in determining the thermodynamic stability of WTe_2 at elevated temperature. Hypothetically, the contributions arising from the lattice vibrations might either result in destabilization of 2H phase or further enhance the stability of 1T′ phase with respect to that of 2H phase upon annealing WTe_2 to high temperature, which could subsequently be an interpretation of why the experimental synthesis of 2H−WTe_2 under pressure has so far never been successfully accomplished. This puts in question the relative stability of Td, 1T′, and 2H phases of WTe_2, not only under high pressure, but also at high temperature, thus deserving further clarification.

In the present work, we perform first-principles calculations, based on the density functional theory, to examine the thermodynamic stability as a function of temperature and pressure of the three WTe_2 polytypes. The influence, arising particularly from the phonons, are taken into account in evaluating the relative stability of WTe_2 at the quasiharmonic level. The results demonstrate that, $p \gtrsim 11$ GPa depending on the temperature, 2H−WTe_2 is the thermodynamically stable with respect to the other two polytypes and its constituent elements. As indicated by no imaginary phonon frequency at $p = 0$ GPa, 2H−WTe_2 is expected to remain metastable also at ambient conditions. We further reveal that the stability of 1T′−WTe_2 is comparable to that of Td−WTe_2 at relevant temperature and pressure, suggesting the coexistence of the two polytypes in any practical samples of WTe_2. These findings provide crucial information for fundamentally understanding the thermodynamic behavior of the compound at a given temperature and pressure.

METHODOLOGY

First-principles calculations

The static total energy E at $T = 0$ K as a function of volume V of the three WTe_2 polytypes and also of tungsten (bcc−W) and tellurium (Te−I, Te−II, or Te−III) considered as relevant competing phases of WTe_2 (see section 3.1 for further details) is derived from the density functional theory (DFT) [12, 13]. Here, the DFT calculations are performed *via* the projector augmented wave (PAW) method [14], as implemented in the Vienna *ab initio* simulation package (VASP) [15, 16], and the generalized gradient approximation (GGA), as proposed by Perdew, Burke, and Ernzerhof [17], is chosen to interpret the exchange−correlation interactions. The energy cutoff for plane waves, included in the expansion of wave functions, is set to be 500 eV, and the Monkhorst−Pack **k**−point mesh [18] is utilized for the Brillouin-zone integration. The correction, as proposed by Grimme (DFT-D3) [19], and the effect of spin-orbit coupling (SOC) are included in all DFT calculations in order to account for the van der Waals interactions, weakly binding adjacent WTe_2 layers, and for the effect of SOC having been reported to be robust for WTe_2 [20], respectively. The details of implementation of the SOC, together with the PAW method, in the VASP code can be found elsewhere [21].

For each considered phase, the optimal equilibrium volume V_0 at $T = 0$ K, minimizing the total energy E, is determined by the minimum point of the E−V curve, derived from a set of E evaluated at different fixed volume V. During the calculations of the energy E at each fixed volume V, the unit-cell shape and all internal atomic coordinates within the cell are allowed to relax, so that the total force acting on each atom is less than 10^{-6} eV/Å. In addition, for all considered phases, calculated $E(V)$ are assured to be converged within an accuracy of 1 meV/f.u. with respect to the plane-wave energy cutoff and the density of the **k**-point grids.

Thermodynamic stability calculations

The relative thermodynamic stability of the three polytypes of WTe_2 at different fixed pressure p and temperature T, in the present work, evaluated through the minimization of the Gibbs free energy $G(T, p)$;

$$G(T, p) = E(V) + F_{vib}(T, V) + pV. \quad (1)$$

For a given polytype of WTe_2, $E(V)$ is the total energy at $T = 0$ directly obtained from the DFT calculations, and $F_{vib}(T,V)$ is the Helmholtz free energy contributed

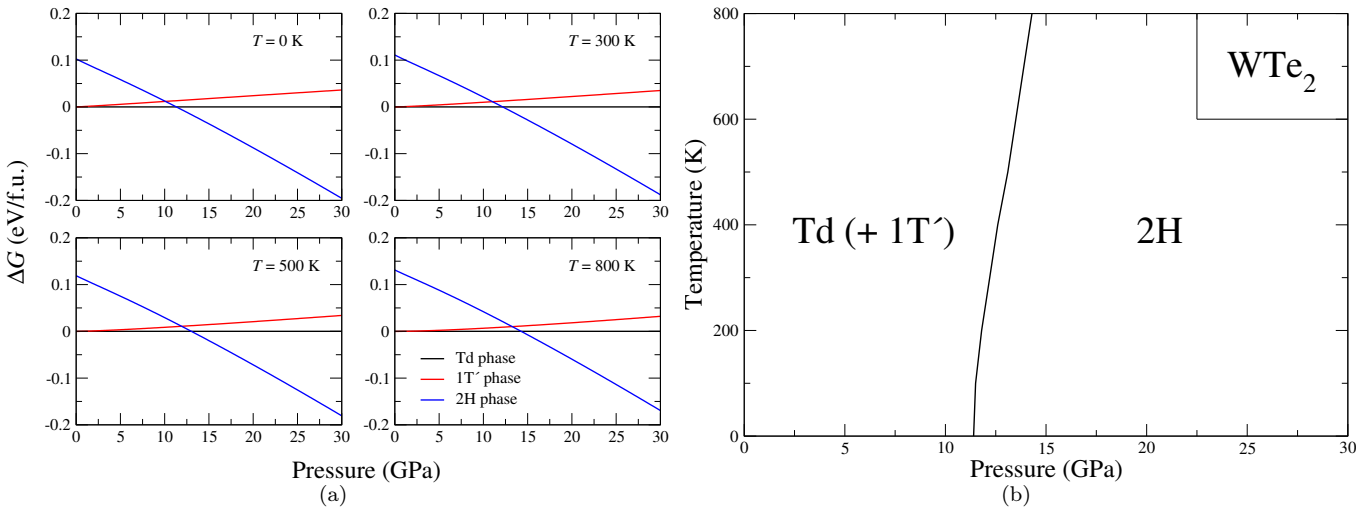

FIG. 2: (a) Gibbs free energy as a function of pressure ranging from 0 GPa to 30 GPa of 1T′−WTe_2 and 2H−WTe_2, evaluated relative to that of Td−WTe_2 at T = 0, 300, 500, and 800 K. (b) p−T phase diagram at a given composition of WTe_2 (see the main text for description).

by the lattice vibrations, given by;

$$F_{vib}(T,V) = \frac{1}{2}\sum_{\mathbf{q},\nu}\hbar\omega(\mathbf{q},\nu,V) + k_BT\sum_{\mathbf{q},\nu}\ln[1-\exp(-\hbar\omega(\mathbf{q},\nu,V)/k_BT)]. \quad (2)$$

ω(**q**,ν,V) denotes the phonon frequency at the wave vector **q** and the band index ν. $\hbar$ and k_B are, respectively, defined as the reduced Planck constant and the Boltzmann constant. It is worth noting that, in addition to **q** and ν, the phonon frequencies ω in Eq. 2 are volume dependent, as the phonon calculations are performed at the quasi-harmonic level using the PHONOPY package for phonon calculations [22, 23], in which the Parlinski-Li-Kawazoe method [24] with a finite displacement of 0.01 Å is employed to calculate the force constants within sufficiently large supercells (96 atoms). Those are, 4×2×1 supercells for Td−WTe_2 and 1T′−WTe_2, and 4×4×1 supercells for 2H−WTe_2. The supercells are then sampled with the 35×35×35 Monkhorst-Pack **k**-point grids in order to guarantee the convergence of the derived phonon frequency ω(**q**,ν,V) and thus the vibrational free energy F_{vib}(T,V). At a given temperature, the term pV as part of the contributions to $G(T, p)$ can be obtained by fitting the sum of the energies $E(V)$ and F_{vib}(T,V) at different fixed volumes to the third-order Birch-Murnaghan equation of state (EOS) [25, 26], and thus the pressure p can thus be derived from;

$$p = -\left[\frac{\partial[E(V)+F_{vib}(T,V)]}{\partial V}\right]_T. \quad (3)$$

Recently, it has been demonstrated that, at high temperature, $F_{vib}(T, V)$ estimated within the quasiharmonic approach can be less quantitatively due to increasingly strong anharmonicity of the lattice vibrations [27]. Given that WTe_2 incongruently melts at $T \approx 1293$ K at ambient pressure [28], the range of temperature in which the temperature-dependent vibrational contributions to $G(T, p)$ are derived in the present work, will be limited not to exceed T = 800 K. That is, less than 2/3 of the melting temperature of the material at ambient pressure. Within such a relatively low temperature range, the anharmonic effect is expected to be negligible and thus the quasiharmonic approximation should be valid for considering the thermodynamic stability of WTe_2.

RESULT AND DISCUSSION

Thermodynamic stability of 2H−WTe_2

By employing the methodologies described in section 2, we determine the Gibbs free energy as a function of pressure and temperature of Td, 1T′, and 2H polytypes of WTe_2. Fig. 2(a) illustrates the Gibbs free energy G of the three WTe_2 polytypes, where 0 GPa $\leqslant p \leqslant$ 30 GPa and T = 0, 300, 500, 800 K. Our results reveal that, in spite of including the influence of lattice vibrations, 2H−WTe_2 is thermodynamically stable with respect both to Td−WTe_2 and to 1T′−WTe_2 at $p \approx 11.5$, 12.3, 13.2, and 14.4 GPa for T = 0, 300, 500, and 800 K, respectively. This is in fact in line with the prediction, previously carried out by Lu *et al.* [7] showing that, without the inclusion of the temperature-dependent ef-

fects, 2H−WTe_2 is thermodynamically favored over the other two phases at $p \gtrsim 10$ GPa. From minimization of the derived Gibbs free energy G at different fixed pressure p and temperature T, we construct a p−T phase diagram (see Fig. 2(b)) to illustrate the relative stability between the three WTe_2 polytypes. Firstly, we consider 2H−WTe_2, and as can be seen from Fig. 2(b), the pressure, at which WTe_2 undergoes a structural phase transition to 2H phase, increases almost linearly with the increase of the temperature. These results suggest that, for a given pressure, the stability of 2H phase tends to decrease upon annealing WTe_2 to higher temperature, which can directly be attributed to the stronger influence of lattice vibrations.

Despite being subject to the high temperature annealing, 2H−WTe_2 should according to the present prediction be stabilized, if the applied pressure is sufficiently large. As we briefly mentioned in section 1, the attempts to synthesize 2H−WTe_2 under high pressure were previously made by Zhou *et al.* [11] and by Lu *et al.* [7]. Nevertheless, in both cases, no successful synthesis of 2H−WTe_2 could be achieved. In case of Ref. [7], two experimental syntheses of 2H−WTe_2 were set up: first, WTe_2 was compressed in the diamond anvil cell (DAC) at $p = 15.4$ GPa and then laser-heated at $T > 2000$ K, and second, WTe_2 was compressed in the DAC at $p = 22.9$ GPa and it was externally resistance-heated at $T = 450$ K. As for the first case, in which the laser-heated DAC technique was employed, our results, derived from the quasiharmonic approach, suggest that the pressure of at least ∼19 GPa is required to stabilize 2H−WTe_2 at $T > 2000$ K, while for the second case, even though the applied pressure of 22.9 GPa is high enough to stabilize 2H−WTe_2 in thermodynamic equilibrium, the annealing temperature of 450 K is somewhat low. By taking into consideration the fact that the temperature of above ∼1000 K and also sufficiently long equilibration time are generally required to achieve high-quality macroscopic crystals of WTe_2 [1, 5, 6], such a relatively low annealing temperature is likely to result in slow diffusion of W and Te atoms. The sluggish processes at low temperature, together with the limited atomic mobility as the material being compressed under high pressure, may thus be the cause of preventing the material to reach its actual equilibrium state, *i.e.*, 2H−WTe_2. The same situation applies also to the experimental synthesis of 2H−WTe_2 under high pressure, as carried out by Zhou *et al.* [11] probably at room temperature. This analysis is also in line with the findings, reported by Lu *et al.* [7], that the transition barrier between 1T′ (and/or Td) and 2H phases is high ($\gtrsim 0.15$ eV/atom) and may presumably be an explanation of why the formation of 2H−WTe_2 did not take place in the high-pressure experiments of Zhou *et al.* [11] and Lu *et al.* [7].

Through the inspection of the phonon density of states, we find that the phonon frequencies of 2H−WTe_2 are all positive not only under high pressure, but also at $p = 0$ GPa (see Fig. 3 illustrating the phonon density of states of the three polytypes of WTe_2 at $p = 0$ and 15 GPa). These findings apparently indicate the dynamical stability of 2H−WTe_2 at $p = 0$ GPa, and further suggest that 2H−WTe_2, if able to synthesize, would possibly remains metastable at ambient pressure. It is worth noting that our results on the phonon density of states (and the lattice parameters, see TABLE I) of 2H−WTe_2 are in good agreement with those previously reported by Lu *et al.* [7].

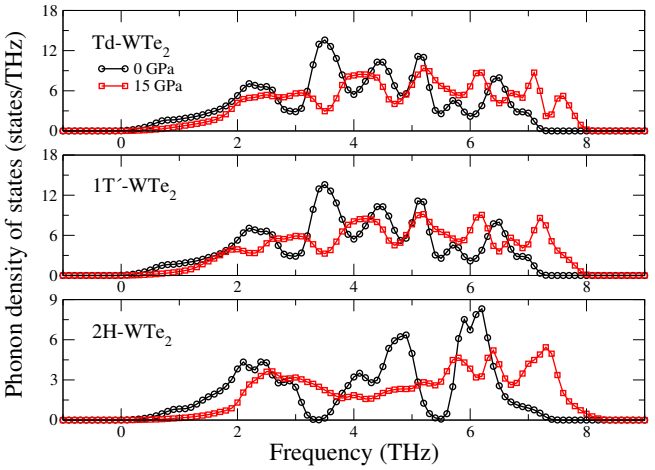

FIG. 3: Phonon density of states of the three WTe_2 polytypes at $p = 0$ and 15 GPa.

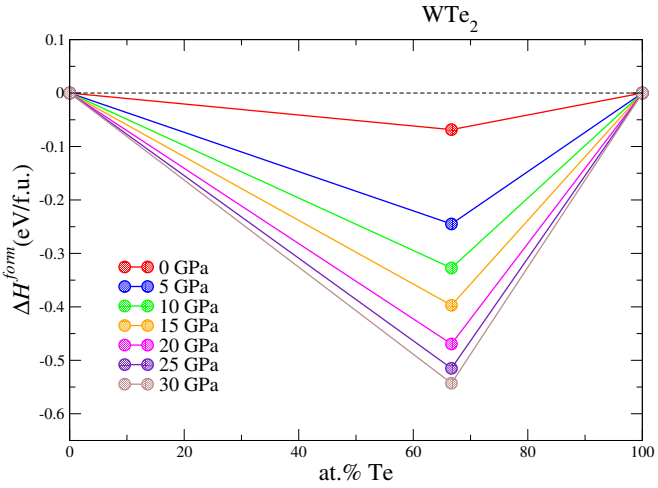

FIG. 4: Formation enthalpy (ΔH^{form}) of WTe_2 as a function of pressure (0 GPa $\leqslant p \leqslant$ 30 GPa), calculated with respect to tungsten and tellurium (see the main text for description).

Although 2H−WTe_2 has been shown to be thermodynamically favored over Td−WTe_2 and 1T′−WTe_2 under high pressure (see Fig. 2), it is no proof that, upon compression to high pressure, the compound will still be stable against phase decomposition into its relevant competing phases. Thus, we evaluate the thermodynamic stability of 2H−WTe_2 with respect not only to Td−WTe_2 and 1T′−WTe_2, but also to its constituent elements in

TABLE I: Optimized lattice parameters (a, b, c) and angles (α, β, γ) of the three WTe_2 polytypes. A comparison is made with the experimental data [9], obtained from single-crystal x-ray diffraction measurements.

Polytype	Lattice parameters a, b, c (Å)	Angles α, β, γ (deg)	References
Td−WTe$_2$	6.284, 3.473, 14.056	90.00, 90.00, 90.00	This work
	6.282, 3.496, 14.070	90.00, 90.00, 90.00	[9]
1T′−WTe$_2$	6.279, 3.469, 14.134	90.00, 89.91, 90.00	This work
2H−WTe$_2$	3.512, 3.512, 14.097	90.00, 90.00, 120.00	This work

order to clarify such an issue. Note that, since pressure is particularly the variable of interest, we neglect at the moment the temperature-dependent effects and as a consequence the Gibbs free energy G, given in Eq. 1, reduces to the enthalpy H;

$$H(p) = E(V) + pV, \tag{4}$$

where the expression of pressure p, given in Eq. 3, is now written as;

$$p = -\frac{\partial E(V)}{\partial V}. \tag{5}$$

The thermodynamic stability of WTe_2 at a given pressure p (and at $T = 0$ K) can then be determined *via* the formation enthalpy ΔH^{form} with respect to tungsten (bcc−W) and tellurium (Te−I, Te−II, or Te−III depending on which pressure is being considered [29]), where the enthalpies H as a function of pressure p of WTe_2 and its constituent elemental phases are calculated from Eq. 4. Fig. 4 illustrates ΔH^{form} as a function of pressure ranging from 0 GPa to 30 GPa of 2H−WTe_2 for which $p \gtrsim 11$ GPa, and (for completeness) also of Td−WTe_2 for which $p < 11$ GPa. Our results show that ΔH^{form} of WTe_2 is negative for all pressures considered here (see Fig 4). This evidently confirms the stability of WTe_2 against decomposition into the constituent elements under pressure up to at least 30 GPa. Interestingly, the formation enthalpy of WTe_2 with respect to its constituent elements becomes more negative upon increasing pressure. This can be attributed to strong interatomic interactions between W and Te atoms in WTe_2 resulting in a negative volume of mixing. That is, the actual volume per formula unit of WTe_2 is smaller than that derived from the sum of the initially separate volumes per atom of W and Te. According to our calculations, the volume of mixing is negative for WTe_2 even at high pressure (up to at least 30 GPa), further stabilizing the compound under pressure.

Relative thermodynamic stability between Td−WTe$_2$ and 1T′−WTe$_2$

In this section, we consider the relative thermodynamic stability between Td−WTe_2 and 1T′−WTe_2. It is worth

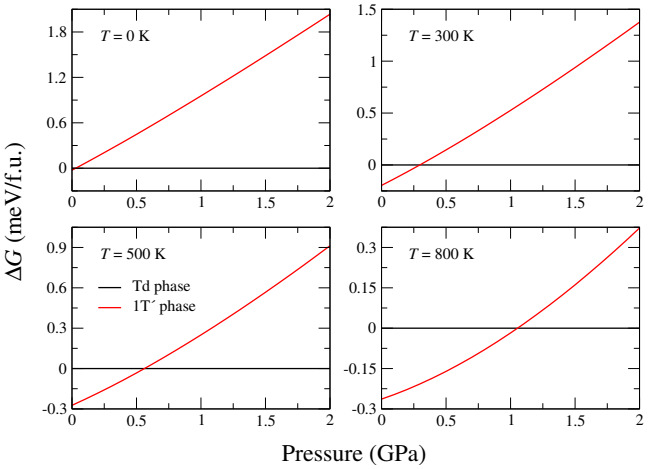

FIG. 5: Gibbs free energy of 1T′−WTe_2, focusing on the low-pressure regions in Fig. 2(a) ($\leqslant 2$ GPa) and evaluated relative to that of Td−WTe_2 at $T = 0$, 300, 500, and 800 K.

mentioning again that, at ambient conditions, Td−WTe_2 has been reported in the literature [9, 10] and accepted to be the most stable WTe_2 polytype. According to our prediction shown in Fig. 2(a), the Gibbs free energy G of 1T′−WTe_2 in particular at low pressure is, however, very close to that of Td−WTe_2. We notice that the similarity between the two polytypes in terms of enthalpy H at low pressure was previously reported by Lu *et al.* [7]. According to their prediction [7], the enthalpy H of 1T′−WTe_2 becomes lower than that of Td−WTe_2 at $p \gtrsim 4$ GPa, and the enthalpy difference ΔH between the two polytypes at $p = 30$ GPa is only ∼5 meV/atom. On the other hand, our prediction reveals that, regardless of temperature, the Gibbs free energy G of 1T′−WTe_2 relative to that of Td−WTe_2 tends to increase upon increasing the pressure, as can be seen from Fig. 2(a). The difference in the relative stability between the two WTe_2 polytypes between our work and that of Lu *et al.* [7] may be attributed either to the difference in the exchange-correlation functional and also the correction to account for the van der Waals interactions, employed between the two studies or to the absence of the influence of thermally excited lattice vibrations in the work of Lu *et al.* [7]. We additionally observe that, within the low-pressure region of Fig. 2(a), there exists a pressure range, in which 1T′−WTe_2 is predicted to be stable with respect to Td−WTe_2, see Fig. 5

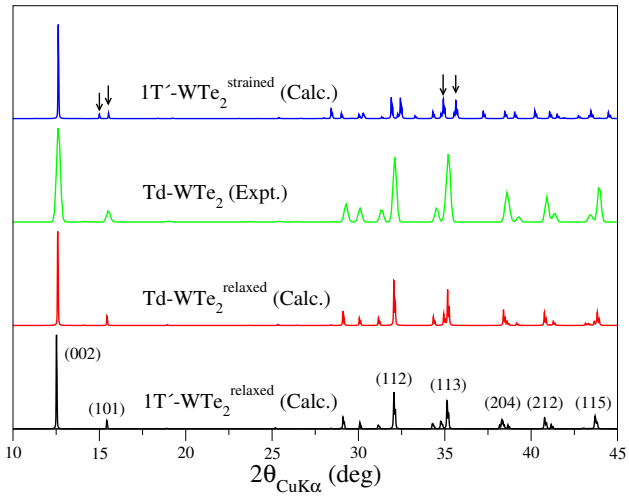

FIG. 6: Simulated x-ray powder-diffraction pattern (Cu$K\alpha$) of Td$-$WTe$_2$ and of 1T$'-$WTe$_2$, obtained from RIETAN$-$FP package [30] as implemented in VESTA [31]. A comparison is made with the existing experimental powder-diffraction data of Td$-$WTe$_2$ [9] (see the main text for description).

showing the Gibbs free energy G of 1T$'-$WTe$_2$, evaluated relative to Td$-$WTe$_2$, within the aforementioned region ($p \leqslant 2$ GPa). Nevertheless, it must be underlined that, despite the prediction of 1T$'-$WTe$_2$ being favored over Td$-$WTe$_2$, the difference in the Gibbs free energy ΔG between the two polytypes, as predicted in our case, is very tiny less than 1 meV/f.u. This is indeed falling into the accuracy range of the first-principles calculations, having been employed in the present work to derive the Gibbs free energy G of WTe$_2$. Moreover, near the boundary at which WTe$_2$ undergoes the transition to 2H polytype, the difference in the Gibbs free energy G between Td$-$WTe$_2$ and 1T$'-$WTe$_2$ is rather small, *i.e.*, $\sim$5 meV/atom at T = 0 K and decreasingly so at higher temperature.

By investigating the optimized lattice parameters both of Td$-$WTe$_2$ and of 1T$'-$WTe$_2$, we observe that the two WTe$_2$ polytypes exhibit very similar lattice parameters, as can be seen from TABLE I. Note also that the monoclinic angle β of 1T$'-$WTe$_2$, after structural relaxation, is estimated to be 89.91 degree, slightly different from that of Td$-$WTe$_2$ only by 0.1%. In the case of Td$-$WTe$_2$, our calculated lattice parameters are in excellent agreement with the experimental data available in the literature (see TABLE I), justifying the reliability of our methodological approaches in terms of exchange-correlation approximation and correction to the total energy due to the van der Waals interactions. This correspondingly results in similarity in the simulated x-ray powder diffraction patterns between Td$-$WTe$_2$ and 1T$'-$WTe$_2$ as denoted, respectively, by Td$-$WTe$_2{}^{relaxed}$ and 1T$'-$WTe$_2{}^{relaxed}$ both depicted in Fig. 6. For comparison to the diffraction patterns of structurally relaxed Td$-$WTe$_2$ and 1T$'-$WTe$_2$, obtained from the simulations, the experimental diffraction data of Td$-$WTe$_2$ [9] is included also in Fig. 6.

Despite the similarities between the two polytypes of WTe$_2$, pointed out above, Lu *et al.* [7] and Zhou *et al.* [11] demonstrated, upon applying pressure, Td$-$WTe$_2$ underwent a phase transition to 1T$'-$WTe$_2$ at $p \gtrsim 4$ GPa. According to their x-ray diffraction studies on WTe$_2$ [7, 11], Td$-$WTe$_2$ and 1T$'-$WTe$_2$ were distinguishable through, *e.g.*, the splitting of (101) and (113) peaks, as the pressure of higher than $\sim$4 GPa was applied to WTe$_2$. Theoretically, we find that such peak splitting can be achieved, when the angle β either of Td$-$WTe$_2$ or of 1T$'-$WTe$_2$ significantly deviates from 90.00 degree due, for instance, to the shear strain applying to the compound along the a axis. Fundamentally, this is associated with the lateral sliding of adjacent WTe$_2$ layers. To verify our statement, we apply the tensile shear strain of 4.5% along the xz direction to 1T$'-$WTe$_2$, as an example, so that the angle β changes from 89.91 to 87.35 degree, and then extract the simulated x-ray diffraction patterns out of it. As shown in Fig. 6, the simulated x-ray diffraction patterns of *strained* 1T$'-$WTe$_2$ reveal the splitting of (101) and (113) peaks, which are both in line with the experimental observations [7, 11]. Such splitting of (101) and (113) peaks is also observed for *strained* Td$-$WTe$_2$ (*not shown*). Lu *et al.* [7] recently showed *via* their theoretical simulations that the transition barrier for sliding the layers of WTe$_2$ relative to each other, induced by the shear strain, is typically small (less than 1 meV/atom). Such a low barrier indicates that, upon being compressed under high pressure, the WTe$_2$ layers of Td$-$WTe$_2$ and of 1T$'-$WTe$_2$ tend to easily and systematically slip with respect to each other, thus resulting in the splitting of (101) and (113) peaks as observed in the experiments [7, 11]. As shown in Fig. 3, both Td$-$WTe$_2$ and 1T$'-$WTe$_2$ are dynamically stable at $p = 0$ and under high pressure, implying that the two polytypes can exist as a metastable phase upon being compressed at relatively low temperatures, at which the atomic mobility and diffusion of both W and Te atoms are kinetically limited [7, 11].

These analyses, based on our findings showing the substantial similarities between Td$-$WTe$_2$ and 1T$'-$WTe$_2$ in terms of thermodynamic stability and of structural behavior, suggest not only that, for a given pressure and temperature within an area, labeled by "Td (+ 1T$'$)" in the $p-T$ phase diagram of WTe$_2$ (Fig. 2(b)), the two polytypes may coexist in practical samples of WTe$_2$ due probably to grains/regions either with tiny difference in stress, for example, or with different growth history, but also that the designation of 1T$'$ polytype, having been used in the literature to described the compound under pressure [7, 11], might actually be represented by a mixture of *strained* Td$-$WTe$_2$ and *strained* 1T$'-$WTe$_2$. This, however, poses a challenge to distinguishing the two polytypes in practice, thus requiring further experimental elaborations.

CONCLUSION

In this work, we investigate through first-principles calculations the thermodynamic stability of the three phases of WTe_2 as a function of pressure and temperature, where the temperature-dependent contributions, arising particularly from the lattice vibrations, are obtained within the quasiharmonic approximation. Our calculated results reveal that, the critical pressure triggering the structural phase transition in WTe_2 to 2H phase increases almost linearly with the increase of the temperature. For example, at $T = 0$ K, 2H$-WTe_2$ is thermodynamically favored over Td$-WTe_2$ and 1T$'-WTe_2$ at $p \approx 11.5$ GPa, while p of at least ~ 14.4 GPa is required to stabilize 2H$-WTe_2$ at $T = 800$ K. We investigate the phonon density of states of 2H$-WTe_2$, and find that it is dynamically stable even at $p = 0$ GPa, implying that 2H$-WTe_2$, if able to synthesize, would remain as a metastable phase also at ambient conditions. Our investigation further reveals the considerable similarities between Td$-WTe_2$ and 1T$'-WTe_2$ in terms of stability and crystal structure, indicating that the two polytypes are likely to coexist in practical samples of WTe_2, as those samples might include grains/regions with tiny difference in stress or with different growth history. Also, our analyses on the structural behavior of Td$-WTe_2$ and of 1T$'-WTe_2$ suggest that the designation of 1T$'-WTe_2$, having been regularly used in the literature to described the compound under high pressure ($p \gtrsim 4$ GPa), might actually be a mix phase of Td$-WTe_2$ and 1T$'-WTe_2$, whose WTe_2 layers laterally slide owing probably to the applied pressure, resulting in significant deviation of the angle β from 90.00 degree and thus the splitting of (101) and (113) peaks as observed in the experiments [7, 11].

Acknowledgements

A. E. acknowledges the supports from the Thailand Toray Science Foundation (TTSF) and Ratchadaphiseksomphot Endowment Fund, Chulalongkorn University; Grants for Research (CU−GR_62_66_23_26). N. K. acknowledges the support from Ratchadaphiseksomphot Endowment Fund, Chulalongkorn University; Grants for Development of New Faculty Staff and the Research Fund for DPST Graduate with First Placement (Grant No. 003/2015), The Institute for the Promotion of Teaching Science and Technology (IPST), Thailand. B.A. acknowledges financial support from the Swedish Government Strategic Research Area in Materials Science on Functional Materials at Linköping University, Faculty Grant SFOMatLiU No. 2009 00971, as well as support from the Swedish Foundation for Strategic Research through the Future Research Leaders 6 program, FFL 15-0290, from the Swedish Research Council (VR) through the grant 2019-05403, and Knut and Alice Wallenberg Foundation (Wallenberg Scholar Grant No. KAW-2018.0194). All of the calculations are carried out using supercomputer resources provided by the Swedish National Infrastructure for Computing (SNIC) performed at the National Supercomputer Centre (NSC).

* Electronic address: noravee.k@chula.ac.th

[1] M. N. Ali, J. Xiong, S. Flynn, J. Tao, Q. D. Gibson, L. M. Schoop, T. Liang, N. Haldolaarachcige, M. Hirschberger, N. P. Ong, and R. J. Cava. Large, non-saturating magnetoresistance in WTe_2. *Nature*, 514:205, 2014.

[2] A. A. Soluyanov, D. Gresch, Z. Wang, Q.-S. Wu, M. Troyer, X. Dai, and B. A. Bernevig. Type-II Weyl semimetals. *Nature*, 527:495, 2015.

[3] F. Y. Bruno, A. Tamai, Q. S. Wu, I. Cucchi, C. Barreteau, A. de la Torre, S. McKeown Walker, S. Riccò, Z. Wang, T. K. Kim, M. Hoesch, M. Shi, N. C. Plumb, E. Giannini, A. A. Soluyanov, and F. Baumberger. Observation of large topological trivial Fermi arcs in the candidate type-II Weyl semimetal WTe_2. *Physical Review B*, 94:121112(R), 2016.

[4] C. Wang, Y. Zhang, J. Huang, S. Nie, G. Liu, A. Liang, Y. Zhang, B. Shen, J. Liu, C. Hu, Y. Ding, D. Liu, Y. Hu, S. He, L. Zhao, L. Yu, J. Hu, J. Wei, Z. Mao, Y. Shi, X. Jia, F. Zhang, S. Zhang, F. Yang, Z. Wang, Q. Peng, H. Weng, X. Dai, Z. Fang, Z. Xu, C. Chen, and X. J. Zhou. Observation of Fermi arc and its connection with bulk states in the candidate type-II Weyl semimetal WTe_2. *Physical Review B*, 94:241119(R), 2016.

[5] X.-C. Pan, X. Chen, H. Liu, Y. Feng, Z. Wei, Y. Zhou, Z. Chi, L. Pi, F. Yen, F. Song, X. Wan, Z. Yang, B. Wang, G. Wang, and Y. Zhang. Pressure-driven dome-shaped superconductivity and electronic structural evolution in tungsten ditelluride. *Nature Communications*, 6:7805, 2015.

[6] D. Kang, Y. Zhou, W. Yi, C. Yang, J. Guo, Y. Shi, S. Zhang, Z. Wang, C. Zhang, S. Jiang, A. Li, K. Yang, Q. Wu, G. Zhang, L. Sun, and Z. Zhao. Superconductivity emerging from a suppressed large magnetoresistant state in tungsten ditelluride. *Nature Communications*, 6:7804, 2015.

[7] P. Lu, J.-S. Kim, J. Yang, H. Gao, J. Wu, D. Shao, B. Li, D. Zhou, J. Sun, D. Akinwande, D. Xing, and J.-F. Lin. Origin of superconductivity in the Weyl semimetal WTe_2 under pressure. *Physical Review B*, 94:224512, 2016.

[8] S. Manzeli, D. Ovchinnikov, D. Pasquier, O. V. Yazyev, and A. Kis. 2D transition metal dichalcogenides. *Nature Review Materials*, 2:17033, 2017.

[9] B. E. Brown. The crystal structures of WTe_2 and high-temperature of $MoTe_2$. *Acta Crystallographica*, 20:268, 1966.

[10] C.-H. Lee, E. Cruz-Silva, L. Calderin, M. A. T. Nguyen, M. J. Hollander, B. Bersch, T. E. Mallouk, and J. A. Robinson. Tungsten ditelluride: a layered semimetal. *Scientific Reports*, 5:10013, 2015.

[11] Y. Zhou, X. Chen, N. Li, R. Zhang, X. Wang, C. An, Y. Zhou, X. Pan, F. Song, B. Wang, W. Yang, Z. Yang, and Y. Zhang. Pressure-induced Td to 1T$'$ structural phase transition in WTe_2. *AIP Advances*, 6:075008, 2016.

[12] P. Hohenberg and W. Kohn. Inhomogeneous electron gas.

Physical Review, 136.3B:864, 1964.

[13] W. Kohn and L. J. Sham. Self-consistent equations including exchange and correlation effects. *Physical Review*, 140:A1133, 1965.

[14] P. E. Blöchl. Projector augmented-wave method. *Physical Review B*, 50(24):17953, 1994.

[15] G. Kresse and J. Furthmüller. Efficiency of ab-initio total energy calculations for metals and semiconductors using a plane-wave basis set. *Computational Materials Science*, 6:15, 1996.

[16] G. Kresse and J. Furthmüller. Efficient iterative schemes for *ab initio* total-energy calculations using a plane-wave basis set. *Physical Review B*, 54:11169, 1996.

[17] J. Perdew, K. Burke, and M. Ernzerhof. Generalized Gradient Approximation Made Simple. *Physical Review Letters*, 77:3865, 1996.

[18] H. J. Monkhorst and J. D. Pack. Special points for Brillouin-zone integrations. *Physical Review B*, 13:5188, 1976.

[19] S. Grimme, J. Antony, S. Ehrlich, and S. Kreig. A consistent and accurate *ab initio* parametrization of density fucntional dispersion correction (DFT-D) for the 94 elements H-Pu. *The Journal of Chemical Physics*, 132:154104, 2010.

[20] J. Jiang, F. Tang, X. C. Pan, H. M. Liu, X. H. Niu, Y. X. Wang, D. F. Xu, H. F. Yang, B. P. Xie, F. Q. Song, P. Dudin, T. K. Kim, M. Hoesch, P. Kurmar Das, I. Vobornik, X. G. Wan, and D. L. Feng. Signature of strong spin-orbit coupling in the large nonsaturating magnetoresistance material WTe_2. *Physical Review Letters*, 115:166601, 2015.

[21] S. Steiner, S. Khmelevskyi, M. Marsmann, and G. Kresse. Calculations of the magnetic anisotropy with projected-augmented-wave methodology and the case study of disordered $Fe_{1-x}Co_x$ alloys. *Physical Review B*, 93:224425, 2016.

[22] A. Togo and I. Tanaka. First principles phonon calculations in material science. *Scripta Materialia*, 108:1, 2015.

[23] A. Togo, F. Oba, and I. Tanaka. First-principles calculations of the ferroelastic transition between rutile-type and $CaCl_2$-type SiO_2 at high pressures. *Physical Review B*, 78:134106, 2008.

[24] K. Parlinski, Z. Q. Li, and Y. Kawazoe. First-principles determination of the soft mode in cubic ZrO_2. *Physical Review Letters*, 78:4063, 1997.

[25] F. D. Murnaghan. On the theory of the tension of an elastic cylinder. *Proceeding of the National Academy of Sciences of the United States of America*, 30:382, 1944.

[26] F. Birch. Finite elastic strain of cubic crystals. *Physical Review*, 71:809, 1947.

[27] P. Korotaev, M. Belov, and A. Yanilkin. Reproducibility of vibrational free energy by different methods. *Computational Materials Science*, 150:47, 2018.

[28] S. Song, S.-Y. Kim, J. Kwak, Y. Jo, J. H. Kim, J. H. Lee, J.-U. Lee, J. U. Kim, H. D. Yun, Y. Sim, J. Wang, D. H. Lee, S.-H. Seok, T. Kim, H. Cheong, Z. Lee, and S.-Y. Kwon. Electrically robust single-crystalline WTe_2 nanobelts for nanoscale electrical interconnects. *Advanced Science*, 6:1801370, 2018.

[29] C. Hejny, S. Falconi, L. F. Lundegaard, and M. I. McMahon. Phase transitions in tellurium at high pressure and temperature. *Physical Review B*, 74:174119, 2006.

[30] F. Izumi and K. Momma. Three-dimensional visualization in powder diffraction. *Solid State Phenomena*, 130:15, 2007.

[31] K. Momma and F. Izumi. *VESTA 3* for three-dimensional visualization of crystal, volumetric and morphology data. *Journal of Applied Crystallography*, 44:1272, 2011.